

Dear Matthias,

We thank you for the constructive comments and for pointing out the shortcomings of the paper. Below, please find point by point answers to your comments.

General remarks:

(1) More uncertainty estimations are needed:

A revised version of the manuscript contains additional error estimations including uncertainty in the a priori H_2^{16}O profile and uncertainties in spectral line intensities and air broadened half-widths.

(2) Clearer discussion of the differences wrt the MUSICA data is needed:

We've clarified that we a posteriori calculate isotopic ratios from the retrieved H_2^{16}O , H_2^{18}O and HDO columns. We also discuss in the introduction that MUSICA dD products are well characterized and currently the best remotely-sensed dD products available.

Detailed remarks:

(1) The title is misleading since the authors retrieve H216O, H218O, and HD16O and not $\delta^{18}\text{O}$ and δD ! The title needs to be modified accordingly. I propose:

"Aposteriori calculation of $\delta^{18}\text{O}$ and δD in atmospheric water vapour from ground-based FTIR retrievals of H216O, H218O, and HD16O"

We agree and accept the new title.

(2) Similar to (1): in the abstract the authors talk about retrieved $\delta^{18}\text{O}$ and δD or $\delta^{18}\text{O}$ and δD retrievals. I think it is important to make clear that the ratios are calculated after the retrieval process, since the aposteriori calculation is an important error source.

Please see the updated version of the manuscript after the comments.

(3) Page 204 last line to page 205 line 2: The authors should not try selling a drawback as an advantage: If you scale a profile, but your spectrum contains

information about the profile shape, your result will depend on the assumed a priori profile shape.

The part containing the GGG suite description was removed from the paper by the request of the second reviewer.

(4) Page 205 line 4 and Fig. 5: what is the weighting function? Is it the Jacobian (dy/dx) or the gain function (dx/dy). I am more used to averaging kernels. Maybe it is possible to plot the averaging kernels?

A revised version of the manuscript contains plots of column averaging kernels of H_2^{16}O , H_2^{18}O and HDO.

(5) Eqs. (3) and (4): STD between ECHAM and the simplified "model" of Eqs. (3) and (4) is 35‰ and 4‰, for δD and $\delta 18O$, respectively. That is you need a precision of 35‰ and 4‰! If you do not reach this precision you don't have to measure δD and $\delta 18O$, then you can just calculate it from H_2^{16}O according to Eqs. (3) and (4), right?

Absolutely. We then show that using columnar retrievals of H_2^{18}O and HDO for a posteriori calculations of δD and $\delta 18O$ improves agreement with the model.

(6) Page 208, line 20-23: The authors seem not to account for the averaging kernel when comparing to the model? If yes, this should be mentioned.

We do, but this part was not properly discussed. Now we mention it in the model description and show averaging kernels plots.

(7) Page 208, line 27: The authors seem to perform retrievals for each spectral window independently. This is different to what I know from TCCON and NDACC, where all windows are generally fitted simultaneously. Maybe this difference should be made clear.

As far as we know, the GGG suite handles all spectral windows independently.

(8) Page 209, last paragraph, discussion about potential d-excess product and potential reasons for disagreement with ECHAM: the authors should be more careful when discussing potential d-excess data! According to Fig. 9 the ECHAM d-excess value is within 5-15‰ (signal variation of less than 10‰). In order to detect this small signal the $\delta 18O$ data need to have a precision of almost 1‰! Already the uncertainty due to the a priori assumed relation

between the isotopologues means a $\delta^{18}\text{O}$ uncertainty of 0.5‰ (see page 206, line 15). To that value the authors must add the uncertainty caused by the assumed NCEP a priori profile (an uncertainty estimation which they still need to make ...). Furthermore, there is an uncertainty in δD ...

In general I think the authors need to better take into account the uncertainties due to their a priori assumptions when discussing the differences between their products and the model data.

We decided to remove d-excess from the discussion because uncertainty now is too high.

(9) Fig. 8, 9, 10: Do the measurements really introduce new information? We must remember that the retrieval uses a lot of a priori information and the variation as seen in the calculated δD and $\delta^{18}\text{O}$ might be already seen in the a priori data. The authors should test this: First, they should plot the δD and $\delta^{18}\text{O}$ data as calculated from the retrieved H_2^{16}O according to Eqs (3) and (4). Second, they should investigate if the so-calculated δD and $\delta^{18}\text{O}$ data is really significantly different from the δD and $\delta^{18}\text{O}$ data as calculated from the retrieved H_2^{16}O , H_2^{18}O and HD^{16}O . It might be that it is sufficient to retrieve H_2^{16}O . The authors should answer the question if the H_2^{18}O and HD^{16}O retrievals really add complementary information?

In the revised manuscript we discuss a huge amount of a priori information in the retrievals and we show that using columnar retrievals of H_2^{18}O and HDO introduce complementary information to the results.

A posteriori calculation of $\delta^{18}\text{O}$ and δD in atmospheric water vapour from ground-based FTIR retrievals of H_2^{16}O , H_2^{18}O , and HD^{16}O

Laboratory of Climate and Environmental Physics, Ural Federal University, Russia

Institut Pierre Simon Laplace, Laboratoire des Sciences du Climat et de l'Environnement, France

Atmosphere and Ocean Research Institute, University of Tokyo, Japan

Alfred Wegener Institute for Polar and Marine Research, Germany

Institute of Environmental Physics, Bremen University, Germany

Correspondence to: N. V. Rokotyan (nrokotyan@gmail.com)

Abstract

This paper investigates the feasibility of a posteriori calculations of columnar δD and $\delta^{18}O$ in atmospheric water vapour from high-resolution ground based measurements of atmospheric transmittance spectra in the near-infrared region ($4000\text{--}11\,000\text{ cm}^{-1}$).

5 A set of refined $H_2^{16}O$, $H_2^{18}O$ and HDO spectral windows for a posteriori calculations of δD and $\delta^{18}O$ is presented.

Uncertainty estimations for the a posteriori calculated δD and $\delta^{18}O$ values are provided. These estimations include uncertainties connected with the measurement noise, errors in the a priori data and uncertainties of spectroscopic parameters.

10 Time series of $\delta^{18}O$ obtained from ground-based FTIR spectra are presented for the first time. A comparison with the results of the ECHAM5-wiso isotopic general circulation model (GCM) simulations demonstrates a good agreement and show that retrieval of HDO and $H_2^{18}O$ can introduce additional information to δD and $\delta^{18}O$ values.

1 Introduction

15 Monitoring of isotopic content of water vapour provides a rich information on the water cycle. Heavier water isotopologues, HDO and $H_2^{18}O$, condense more actively and evaporate less actively than the main isotopologue $H_2^{16}O$, due to differences in the saturation vapour pressure of these three molecules. As a result of this equilibrium effect, each cycle of evaporation and condensation generally results in depletion of the air of $H_2^{18}O$ and HDO with increasing
20 depletion as the water vapor mixing ratio, and thus the air mass temperature, decreases. This depletion process affects both $H_2^{18}O$ and HDO with subtle differences owing to the existence of an additional kinetic effect resulting in the differences in the diffusivity of water molecules in air. More specifically the equilibrium effect is 8 to 10 times larger than the kinetic effect for
25 HDO while it is of the same order of magnitude for $H_2^{18}O$. This results in a significant difference in processes occurring far for equilibrium for both isotopologues. In the atmosphere, this

is the case for evaporation of large drops below cloud base and for the formation of ice crystals in a supersaturated environment. When occurring in a given airmass, these processes leave an imprint in the relative change of

Usually, concentration ratios of different isotopologues are expressed in terms of delta-values:

$$\delta^x A = \left(\frac{(n_x/n_a)_{\text{sample}}}{(n_x/n_a)_{\text{standard}}} - 1 \right) \cdot 1000 \text{ [‰]}, \quad (1)$$

where $(n_x/n_a)_{\text{sample}}$ is a measured ratio of the less abundant isotopologue to the most abundant, and $(n_x/n_a)_{\text{standard}}$ is a standard ratio. The Vienna Standard Mean Ocean Water (VSMOW) values are 2005.2×10^{-6} for $^{18}\text{O}/^{16}\text{O}$ and 155.76×10^{-6} for D/H (Craig, 1961). A commonly used approach for inferring information from $\delta^{18}\text{O}$ and δD co-isotopic measurements is through the deuterium-excess defined by Dansgaard (1964) as $d = \delta D - 8 \cdot \delta^{18}\text{O}$.

Thanks to the recent development of methods that allow for the retrieval of information on the distribution of water isotopologues in the atmosphere there is a growing interest of using isotopic data for investigating atmospheric processes controlling tropospheric humidity and stratosphere–troposphere water vapour exchange (Rinsland et al., 1991; Moyer et al., 1996; Coffey et al., 2006; Payne et al., 2007; Nassar et al., 2007).

Due to the difficulty of retrieving information about $\delta^{18}\text{O}$ in atmospheric water vapor, such studies are largely based on deuterium data. Satellite data from different instruments offer complementary information. While ACE and MIPAS give access to δD from the stratosphere to the upper troposphere (Nassar et al., 2007; Risi et al., 2012a, b), TES enables the retrieval of some information on the δD vertical distribution (Worden et al., 2006, 2007), IASI retrieves δD in the mid troposphere, between 1 and 5 km (Schneider and Hase, 2011; Pommier et al., 2013), and SCIAMACHY (Frankenberg et al., 2009) and GOSAT (Boesch et al., 2013; Frankenberg et al., 2013) provide with δD data integrated over the entire atmospheric column.

The ATMOS Fourier transform infrared spectrometer installed on the Space Shuttle was the first instrument used to retrieve information about stratospheric abundances of H_2^{18}O , HDO, H_2^{16}O and their ratios (Rinsland et al., 1991; Kuang et al., 2003; Coffey et al., 2006). Actively developing satellite remote sounding techniques made it possible to obtain spatial and temporal

distributions of δD in the troposphere by a posteriori δD calculations from retrieved $H_2^{16}O$ and HDO concentrations (Gribanov and Zakharov, 1999; Zakharov et al., 2004; Herbin et al., 2007, 2009; Frankenberg et al., 2009, 2013; Boesch et al., 2013) and by applying an optimal estimation strategy to retrieve δD , which produces results not affected by different vertical sensitivities to $H_2^{16}O$ and HDO (Worden et al., 2006, 2007; Schneider and Hase, 2011). The first attempts to obtain tropospheric $\delta^{18}O$ from space were made by (Herbin et al., 2007) using IMG/ADEOS spectra in thermal IR region. However, satellite measurements cannot provide sufficient accuracy and precision to get temporal variations of $\delta^{18}O$ in the atmosphere. Remote sensing of δD from ground-based FTIR instruments was pioneered by Schneider et al. (2006, 2010, 2012) in the thermal infrared and now is under development in the near infrared (Gribanov et al., 2011; Skorik et al., 2013). Routine monitoring of atmospheric $\delta^{18}O$ is limited to in-situ measurements of water vapour isotopic composition at the surface and analysis of precipitation samples (Rozanski et al., 1992; Kerstel et al., 1999; Lee et al., 2005; Steen-Larsen et al., 2013).

Ground-based FTIR remote sounding of atmospheric constituents is now actively used for validation of satellite data and long-term local measurements of the atmospheric composition. The high spectral resolution of such instruments clearly resolves absorption lines of atmospheric species with a good signal to noise ratio suitable for monitoring atmospheric composition. The Total Carbon Column Observing Network (TCCON) (Wunch et al., 2010, 2011) and the Network for the Detection of Atmospheric Composition Change (NDACC) (Hannigan et al., 2009) use FTIR observations for accurate and precise retrievals of CO_2 , CH_4 , H_2O , O_3 , HF, HCl, and other trace gas concentrations in the atmosphere. Retrieving atmospheric methane, carbon dioxide and water vapour abundances from ground-based high-resolution FTIR measurements is a routine procedure that can be done with a precision up to 0.25 % (Wunch et al., 2011). The TCCON community also produces standard products of HDO and $H_2^{16}O$ columnar values, which are often used for a posteriori δD calculations. Though such δD calculations can be affected by the different vertical sensitivity of $H_2^{16}O$ and HDO retrievals, these data were used for intercomparison with LMDZ-iso general circulation model (GCM) simulations (Risi et al., 2012a, b) and GOSAT satellite retrievals (Boesch et al., 2013; Frankenberg et al., 2013). Within the MUSICA project measurements from ten NDACC stations were used for the optimally esti-

mated retrieval of δD vertical distribution in the troposphere (Schneider et al., 2012). MUSICA δD products are well characterized with the detailed documentation of the uncertainties of ratio products and are the best remotely measured δD products currently available. These studies show that a growing network of ground-based FTIR sites can play an important role in future monitoring of the isotopic content of water vapour in the atmosphere. However, a posteriori calculated ratio products are still not well documented.

In this article we focus on a posteriori calculations of δD and $\delta^{18}\text{O}$ using ground-based near infrared columnar retrievals of H_2^{16}O , HDO and H_2^{18}O . As for SCIAMACHY and GOSAT, this technique gives an access to integrated column data and is thus mainly sensitive to the lower troposphere since about 90 % of the atmospheric water is below 500 hPa. Such lower tropospheric data are interesting to understand GCM biases in simulating the water cycle by models equipped with water isotopologues. Using the isotopic version of the LMD model, Risi et al. (2013) have investigated the role of continental recycling, while Gryasin et al. (2013) has suggested that the difficulty of this model in simulating the water cycle over Western Siberia may be due to a problem in the large-scale advection or to insufficient surface evaporation. Also interesting is the fact that, at least in a model world, the δD of the total water column is highly correlated with δD near surface values as shown by Griбанov et al. (2013) for a site in Western Siberia. In turn, such recent studies point both to the usefulness of total column integrated δD , which could be easily extended to the study of seasonal and intraseasonal variations when sufficiently long time series will be available, and to the possibility of comparing and possibly combining such data with in-situ δD measurements in ground level water vapor at sites like Kourouka (Griбанov et al., 2013) where both FTIR and PICARRO measurements are performed. Obviously, getting reliable $\delta^{18}\text{O}$ data would further increase the interest of retrieving total column integrated water isotopologues using FTIR. If sufficient accuracy of the retrieved values of both isotopologues can be achieved one could for example get information about the oceanic origin of an air mass as its water vapor deuterium-excess is influenced by the conditions (humidity, temperature) prevailing in the evaporative source regions (Merlivat and Jouzel, 1979).

2 Spectral window selection

Though there are known H_2^{16}O and HDO spectral windows in near infrared region, which are used by the TCCON community, we decided to look for additional ones that may improve the precision of δD calculations. To our knowledge on H_2^{18}O , there are no reported windows in near infrared region that can be used for the isotopic retrieval.

To select spectral windows we have simulated atmospheric transmittance spectra in a wide spectral range from 4000 cm^{-1} to $11\,000\text{ cm}^{-1}$ by the FIRE-ARMS (Fine Infra-Red Explorer for Atmospheric Remote Measurements) software package (Gribanov et al., 1999, 2001) using a mid latitude summer standard model for the atmospheric state (Anderson et al., 1986). These simulations were then analyzed to identify a number of spectral windows that contain clear signatures of H_2^{16}O , H_2^{18}O and HDO with a little interference by absorption lines linked to other gases.

We have used the GGG (ver.2012) software suite (Wunch et al., 2011) to retrieve columnar concentrations of H_2^{16}O , H_2^{18}O and HDO from the selected spectral windows from spectra recorded at Bremen TCCON site during 2010–2012. We then have analyzed retrieval results from measurements taken under different conditions: various humidity levels, wide atmospheric temperature range (summer and winter measurements) and different solar zenith angles. We have used the following criteria for the spectral windows set refinement: (a) peak value in average fitting residuals shouldn't exceed 1.5 %; (b) correlation between columnar concentrations retrieved from different windows should be higher than 0.9. Refined HDO and H_2^{16}O spectral windows set were then combined with those used in the TCCON community. Usage of additional windows in our retrievals allowed us to improve the accuracy of the a posteriori calculated δD values by 25 % (comparing to the model). Thus the standard deviation of the difference between monthly averaged values of a posteriori calculated δD and ECHAM5-wiso δD has improved from 24 % to 18 %. The full set of the refined H_2^{16}O , H_2^{18}O and HDO windows is presented in Fig. 1 (see Table 1 for summarized information). Fig. 2 shows the column averaging kernels for H_2^{16}O , H_2^{18}O and HDO.

Fig. 3 shows scatter plots (left panels) of daily-averaged δD obtained from publicly available TCCON (a posteriori calculated, varying a priori) and MUSICA/NDACC (optimally estimated, single a priori) retrievals vs. δD obtained by using the refined set of spectral windows. The results are in a good agreement with a correlation coefficient $r = 0.96$ and $r = 0.94$ respectively.

5 Since a lot of δD variations are introduced by the a priori (see section 2), right panel of Fig. 4 shows the same scatter plots with subtracted a priori δD values used for a posteriori calculations of δD and $\delta^{18}O$.

3 Instrumental and retrieval set-up

Since we investigate the feasibility of the retrieval of relative isotopic ratios of water vapour isotopologues from ground-based FTIR measurements in near-infrared that are widely collected by the TCCON network we employed a standard TCCON approach for this task. IR spectral measurements of the cloudless atmosphere registered at the Institute of Environmental Physics (IUP) of the University of Bremen (Germany, 53.104° N, 8.850° E, altitude 27 m, <http://www.iup.uni-bremen.de>) in 2009–2012 were used. IUP is the TCCON site that

15 performs IR measurements in near-infrared region ($4000\text{--}11\,000\text{ cm}^{-1}$) with resolution of 0.02 cm^{-1} . The operating FTIR instrument is a Bruker IFS-125HR with maximum resolution of $9 \times 10^{-4}\text{ cm}^{-1}$. Measurements are collected in DC mode and then processed by a special software to reduce the impact of solar intensity variations caused by cloud and aerosol cover (Keppel-Aleks et al., 2007).

20 The GGG suite implements a scaling retrieval algorithm and the shape of a priori profile can affect accuracy of the retrieval. Initial guess profiles for $H_2^{16}O$ are derived from data of National Centers for Environmental Prediction and the National Center for Atmospheric Research (NCEP/NCAR) (Kalnay et al., 1996). HDO a priori profiles are calculated from $H_2^{16}O$ a priori profiles using the following relationship implemented in the GGG suite:

$$25 \quad x_{\text{HDO}}^{\text{apr}}(h) = 0.16 \cdot x_{\text{H}_2^{16}\text{O}}^{\text{apr}}(h) \cdot \left(8.0 + \log_{10} \left(x_{\text{H}_2^{16}\text{O}}^{\text{apr}}(h) \right) \right), \quad (2)$$

where $x_{\text{HDO}}^{\text{apr}}(h)$ is the a priori HDO volume mixing ratio (vmr) profile, $x_{\text{H}_2^{16}\text{O}}^{\text{apr}}(h)$ is the a priori H_2^{16}O vmr profile, h is the altitude. The term $0.16 \cdot \left(8.0 + \log_{10}(x_{\text{H}_2^{16}\text{O}}^{\text{apr}}(h))\right)$ generally ranges between 0.40 (in the stratosphere) and 0.95 (in the troposphere) and qualitatively describes vertical depletion of HDO. According to the ECHAM5-wiso general circulation model simulations
5 (see further below for a model description) Eq. (2) applied to H_2^{16}O vertical profiles approximates δD profiles with a standard deviation of about 35‰ in the lower troposphere.

To construct H_2^{18}O initial guess profiles we've analyzed the output of the ECHAM5-wiso GCM and found that H_2^{18}O profiles can be approximated similar to HDO profiles using the following relationship:

$$x_{\text{H}_2^{18}\text{O}}^{\text{apr}}(h) = 0.008 \cdot x_{\text{H}_2^{16}\text{O}}^{\text{apr}}(h) \cdot \left(126.5 + \log \left(x_{\text{H}_2^{16}\text{O}}^{\text{apr}}(h) \right) \right), \quad (3)$$

. Similar to Eq. (3) the term $0.008 \cdot \left(126.5 + \log(x_{\text{H}_2^{16}\text{O}}^{\text{apr}}(h)) \right)$ ranges between 0.91 and 0.98 and describe H_2^{18}O vertical depletion. Although this approach is based on a limited number of simulations, it is certainly better than assuming a constant vertical profile of the isotopic relative concentration. According to the model Eq. (3) describes $\delta^{18}\text{O}$ vertical profile with a standard deviation of 4‰ in the lower troposphere (vs. 9‰ when using a constant vertical profile). Examples of the constructed $\delta^{18}\text{O}$ and δD a priori profiles are shown in Fig. 4.

Equations (2) and (3) show that a lot of δD and $\delta^{18}\text{O}$ variations are already introduced by the a priori (see. Fig. 5) and the retrieval of HDO and H_2^{18}O makes sense only if a posteriori calculated δD and $\delta^{18}\text{O}$ can reach the precision of at least 35‰ and 4‰ respectively.

The retrieval demonstrates a low sensitivity to the shape of a priori profiles. We’ve compared retrieval results obtained using constant $\delta^{18}\text{O}$ and δD a priori profiles of 0‰ with the results obtained using a priori profiles constructed as described above. Standard deviation between the results is about 0.5‰ for $\delta^{18}\text{O}$ and 3.8‰ for δD . This means that most of the retrieved information about columnar values of $\delta^{18}\text{O}$ and δD comes from spectra and not from a priori assumptions (Fig. 6).

Using single H_2^{16}O a priori profile for all retrievals instead of NCEP reanalysis data results in an average scatter of 8‰ and 6‰ for δD and $\delta^{18}\text{O}$ respectively.

A priori profiles of other atmospheric species were taken from the standard GGG atmospheric model (Wunch et al., 2010).

As mentioned above, the retrieval employs model results from atmospheric simulations using ECHAM5-wiso (Werner et al., 2011), which is the isotope-enhanced version of the atmospheric general circulation model ECHAM5 (Roeckner et al., 2003, 2006; Hagemann et al., 2006). The model considers both stable water isotopologues H_2^{18}O and HDO which have been explicitly implemented into its hydrological cycle (Werner et al., 2011), analogous to the isotope modeling approach used in the previous model releases ECHAM3 (Hoffmann et al., 1998) and ECHAM4 (e.g. Werner et al., 2001). For each phase of “normal” water (vapor, cloud liquid, cloud ice)

being transported independently in ECHAM5, a corresponding isotopic counterpart is implemented in the model code. Isotopologues and “normal” water are described identically in the GCM as long as no phase transitions are concerned. Additional fractionation processes are defined for the water isotope variables whenever a phase change of the “normal” water occurs in ECHAM5, considering equilibrium and non-equilibrium fractionation processes.

ECHAM5-wiso has been validated with observations of isotope concentrations in precipitation and water vapor (Langebroeck et al., 2011; Werner et al., 2011; Griбанov et al., 2013). On a global and European scale, annual and seasonal ECHAM-5-wiso simulation results are in good agreement with available observations from the Global Network of Isotopes in Precipitation, GNIP (IAEA-WMO, 2006). The simulated near-surface isotopic composition of atmospheric water vapor is also in fairly good agreement with recent monthly observations from five different GNIP stations and with a continuous isotope record at Kourovka Observatory, Western Siberia. Model values and measurements agree well with differences in the range of $\pm 10\%$. A comparison of ECHAM5-wiso results with total column averages of HDO determined by the SCIAMACHY instrument on board the environmental satellite ENVISAT (Frankenberg et al., 2009) shows the same latitudinal gradients, but an offset between 20–50% of unknown origin.

In this study, the horizontal model resolution is T63 in spectral space (about $1.9^\circ \times 1.9^\circ$), and model results for Bremen are evaluated at the nearest grid point. Vertical resolution is 31 levels on hybrid sigma-pressure coordinates. The model is forced with prescribed values of present-day insolation and greenhouse gas concentrations (IPCC, 2000), as well as with sea-surface temperatures and sea-ice concentrations according to ERA-40 and ERA-Interim reanalysis data (Uppala et al., 2005; Dee et al., 2011; Berrisford et al., 2009). Every six hours the dynamic-thermodynamic state of the model atmosphere is constrained to observations by implicit nudging (e.g. Krishnamurti et al., 1991; implemented by Rast, 2008), i.e. modeled fields of surface pressure, temperature, divergence and vorticity are relaxed to ERA-40 and ERA-Interim reanalysis fields (Uppala et al., 2005; Dee et al., 2011; Berrisford et al., 2009; data have been obtained from the ECMWF data server). This approach ensures that the large-scale atmospheric flow is correctly represented also at the sub-seasonal time scale. The hydrological cycle in our ECHAM5 setup is fully prognostic and not nudged to reanalysis data. Our simulation starts on 1

September 1957 using an internal model time step of 12 min. Here, we evaluate daily averaged model results through 2010–2012.

In general, the model captures observed temperature and humidity trends in Bremen. Averaged over the years 2010–2012, the difference between modeled and observed daily surface temperatures is less than about $-1\text{ }^\circ\text{C}$. Averaged over the particular days with FTIR measurements, ECHAM5-wiso simulates surface temperatures, which are about $3\text{ }^\circ\text{C}$ colder than the observations. Comparing simulated vertical temperature profiles with the NCEP a priori profiles used for isotope retrieval, we find that, averaged over the days with measurements, column-averaged temperatures according to ECHAM5-wiso are about $0.8\text{ }^\circ\text{C}$ colder than the a priori values. A similar comparison for specific humidity indicates that the total column water vapor simulated by ECHAM5-wiso is about 2 mm (or 26 %) higher than the a priori values according to NCEP. However, this moist bias tends to cancel in the retrieval when isotopic ratios are considered.

For comparison with FTIR, vertical profiles of H_2^{16}O , H_2^{18}O and HDO from the model were smoothed by averaging kernels from the retrieval (according to Gribanov et al., 2013; Wunch et al., 2010) (see Fig. 2), vertically integrated to get total column values and then isotopic ratios were calculated.

4 Uncertainty estimations

4.1 Measurement noise

The FTIR instrument, which is used here, has signal-to-noise ratio (SNR) of about 200 and 900 in the selected HDO and H_2^{18}O windows, respectively. We've estimated how the measurement noise affects the precision of the a posteriori calculated δD and $\delta^{18}\text{O}$. For a such estimation we've simulated atmospheric transmittances by the FIRE-ARMS software in the selected spectral windows with the constant vertical profiles of $-15\text{ }‰$ for $\delta^{18}\text{O}$ and $-200\text{ }‰$ for δD , which are in a range of natural atmospheric abundances of H_2^{18}O and HDO. A normally distributed noise of different magnitudes representing different noise levels was added to the simulated

spectra to imitate real measurements. Then the retrieval of $\delta^{18}\text{O}$ and δD was performed with only one fitting parameter: the scaling factor of the a priori profile of the isotopologue. For a priori profiles of the retrieval we've used the profiles used in the simulation perturbed by a random factor uniformly distributed in the range of 0.5–1.5. This procedure was repeated 100 times for each noise level. The estimation show that the measurement noise introduces an error of about 1 ‰ for δD and 3 ‰ for $\delta^{18}\text{O}$ (see Fig. 7).

4.2 A priori data

Influence of the uncertainty of the vertical temperature profile has also been analyzed. A perturbation of 1 % (2–3 K depending on the altitude) in the temperature profile leads to approximately 3 ‰ and 10 ‰ deviation in the $\delta^{18}\text{O}$ and δD values, respectively.

Another important source of errors in the retrieval is the uncertainty of the a priori H_2^{16}O profile. A comparison of the local meteo measurements in Bremen with the NCEP reanalysis data interpolated to the same level shows an error of 15–20 % in H_2^{16}O concentrations. To estimate the influence of this uncertainty on a posteriori calculated δD and $\delta^{18}\text{O}$ values we've selected several spectra measured in different seasons and completed 500 retrieval runs with perturbed H_2^{16}O profiles. Each level of a priori H_2^{16}O profiles was perturbed by 15 % (with a correlation length of uncertainty of 2.5 km). The estimation show that 15 % uncertainty in the a priori H_2^{16}O profiles introduces an error of about 8 ‰ for δD and 6 ‰ for $\delta^{18}\text{O}$.

4.3 Spectroscopy

Along with the measurement noise and uncertainty in a priori data, which represent random error of the retrieval, there are other error sources that introduce systematic impacts on the retrieved values. The retrieval procedure relies on spectroscopic data while uncertainties in water vapour spectroscopy remain an important problem (Rothman et al., 2013). The uncertainty in line intensities, half widths and coefficients of temperature dependence of air-broadened half width introduces both systematic shifts and temperature-dependent slopes to the retrieval results.

According to the indices of uncertainty in HITRAN 2008 (Rothman et al., 2009), the uncertainty in the intensity of water vapour spectral lines ranges from 5 to 10 %, while uncertainty in air broadening coefficients typically ranges between 2 and 5 %. The uncertainty in the coefficient of temperature dependence of air-broadened half-width ranges between 10 % and 20 %.
5 This error can lead to tangible under- or overestimation of concentration of the species of interest from measurements taken in winter season when atmospheric temperatures are much colder than HITRAN reference temperature.

To see how spectroscopic uncertainties affect the a posteriori calculated δD and $\delta^{18}O$ values we've perturbed spectroscopic parameters of HDO and $H_2^{18}O$ by a \pm value obtained from
10 HITRAN's indices of uncertainty (it is a kind of worst-case estimation) (see Fig. 8). Changing the spectral line intensities by ± 5 % shifts the δD values by approximately 50 % and the $\delta^{18}O$ values by approximately 47 %. It also introduces a change of slope by 0.05 for both cases. This can lead to a temperature-dependent change of the results up to 12 ‰ and up to 2 ‰ for δD and $\delta^{18}O$, respectively

15 A change of ± 2 % of the coefficient of air broadened half width shifts the results by approximately ± 17 % and ± 14 % for δD and $\delta^{18}O$, respectively. A slope between the results changes by 0.01 for δD and by 0.04 for $\delta^{18}O$. This can lead to a temperature-dependent change of the results up to 1.5 ‰ for δD and up to 1 ‰ for $\delta^{18}O$.

20 A change of the coefficient of temperature dependence by 15 % leads up to 0.7 % deviation in the retrieved concentrations of HDO and $H_2^{18}O$ depending on atmospheric temperature. This can lead to a change of 4–5 ‰ in delta values.

Taking into account that in calculations of delta-values participate two isotopologues and that uncertainty range of the water vapour spectroscopic parameters is relatively high, spectroscopic uncertainties can introduce a significant slope to the results.

25 Table 2 summarizes the information from all the uncertainty estimations

4.4 Linelist

In the present study, we use the modified GGG linelist (which is based on HITRAN 2008) (Wunch et al., 2010) with all H_2O lines substituted by UCL08 water linelist (Shillings et al.,

2011). UCL08 is a compilation of experimental data (Jenouvrier et al., 2007; Mikhailenko et al., 2007, 2008; Coudert et al., 2008; Tolchenov and Tennyson, 2008), HITRAN2008 and additional theoretical lines (Barber et al., 2006). Strong lines of the H_2^{16}O , H_2^{18}O and HDO are identical to those in HITRAN2008. The modified line list allowed us to improve the agreement with
5 ECHAM5-wiso for $\delta^{18}\text{O}$ from $r^2 = 0.64$ to $r^2 = 0.82$. However, the agreement between δD values don't change.

As expected, a posteriori calculated columnar values of $\delta^{18}\text{O}$ and δD are shifted comparing the model. The most likely reason for the shifts is spectroscopic uncertainties (see Sect 4.3). We have calculated and corrected the offsets of 58‰ and -23 ‰ between retrieved and modeled
10 $\delta^{18}\text{O}$ and δD correspondingly.

The HITRAN2012 (Rothman et al., 2013), which became available recently, declares more accurate spectroscopic line intensities and half widths. Retrieval results obtained with this new version of HITRAN database have smaller systematic shifts from the model ($+7$ ‰ and -8 ‰ for $\delta^{18}\text{O}$ and δD , respectively) than those obtained with our GGG+UCL08 line list. Conversely,
15 the correlation is smaller and the slope between retrieved and simulated isotopic ratios is further from the expected. These results indicate that improvements in the spectroscopic line parameters has a mixed impact on the isotopic retrievals and therefore needs further investigation.

5 Retrieval results and comparison with simulations

About 6000 spectra recorded from January 2010 to May 2012 at Bremen TCCON site were
20 processed in order to retrieve columnar values of H_2^{16}O , H_2^{18}O and HDO. Each spectral window of the species of interest (see Table 1) was processed independently and the results were filtered and averaged with respect to uncertainty based on spectral residuals. Since the GGG suite uses NCEP/NCAR reanalysis data for vertical profiles of atmospheric temperatures interpolated to local noon for a whole day of measurements, we have used spectra recorded in a time range of
25 local noon time ± 3 h only. We removed from the comparison the days with measurements that cover less than 2 h. An offset correction was applied to the retrieval results in order to remove the shifts due to spectroscopic uncertainties (as described in Sect. 4.4).

While the retrieval results from individual measurements are noisy, values averaged during one month of measurements show seasonal variability of δD and $\delta^{18}\text{O}$ of about 200‰ and 25‰ respectively. As expected, both δD and $\delta^{18}\text{O}$ generally follow the atmospheric temperature. Correlation coefficient between δD , $\delta^{18}\text{O}$ and temperature at surface are 0.88 and 0.89 respectively while correlation coefficient between columnar δD and $\delta^{18}\text{O}$ is 0.86 (Fig. 9).

Fig. 10 shows time-series of the a posteriori calculated “monthly” values of δD and $\delta^{18}\text{O}$ together with the output of the ECHAM5-wiso general circulation model (Werner et al., 2011). The simulations and the values obtained from the FTIR measurements are correlated with $r^2 = 0.91$ for δD and $r^2 = 0.81$ for $\delta^{18}\text{O}$ and scatter with an absolute standard deviation of 17.9‰ and 5.3‰ respectively.

Left panels of Fig. 11 shows scatter plots of the ECHAM5-wiso simulations vs. the δD and the $\delta^{18}\text{O}$ values calculated from the retrieved H_2^{16}O profile by Eqs. (2) and (3). ECHAM5-wiso δD and $\delta^{18}\text{O}$ correlate to the calculated δD and $\delta^{18}\text{O}$ with $r^2 = 0.8$ and $r^2 = 0.76$, respectively.

The fact that a posteriori calculated δD and $\delta^{18}\text{O}$ improves the agreement with the model shows that the near infrared retrievals of H_2O and H_2^{18}O can introduce additional information to the δD and $\delta^{18}\text{O}$ values;

Right panels of Fig. 11 show scatter plots of the ECHAM5-wiso simulations vs. FTIR results. We define “summer” (red) and “winter” (blue) points corresponding to the surface temperatures above 15 °C and below 15 °C respectively. “Summer” slope is equal to 1.21 and 1.41 for δD and $\delta^{18}\text{O}$ respectively, while “winter” slope values are 1.26 and 2.0. “Summer” results also show better r^2 values of 0.95 and 0.98 for δD and $\delta^{18}\text{O}$, respectively. While “winter” r^2 values are much lower: 0.70 for δD and 0.61 for $\delta^{18}\text{O}$. Most likely, the slopes are caused by the uncertainties of spectroscopic line parameters (as described in Sect. 4.4).

6 Conclusions

We have analyzed the feasibility of a posteriori calculations of column-averaged atmospheric $\delta^{18}\text{O}$ and δD from ground-based high-resolution FTIR measurements in near infrared. The er-

ror estimations show the measurement noise and uncertainties in a priori data can introduce a random error of about 12‰ and 18‰ to δD and $\delta^{18}O$ values respectively. While uncertainties in spectroscopic parameters of HDO and $H_2^{18}O$ can introduce a systematic shift of about 72‰ and 66‰ and a temperature-dependent deviation up to 18‰ and 8‰ to a posteriori calculated δD and $\delta^{18}O$ values respectively. It should be noted that these estimations were done by only perturbing the spectroscopic parameters of HDO and $H_2^{18}O$ and do not take into account possible uncertainties in $H_2^{16}O$ line parameters.

We've showed that near infrared retrievals of HDO and $H_2^{16}O$ can introduce complementary information to a posteriori calculated δD and $\delta^{18}O$.

Time series of the atmospheric $\delta^{18}O$ values obtained by remote sensing are presented for the first time. Isotopic ratios obtained from "summer" spectra show a good agreement with the ECHAM5-wiso general circulation model, while the agreement with the retrieval from "winter" spectra is worse (probably because of the lower spectral signal due to much lower water vapour atmospheric concentration). Recent studies also report that Voigt line shape model does not describe the shape of water vapour absorption line perfectly (Boone et al., 2007; Schneider et al., 2011; Schneider and Hase, 2011) and usage of the speed-dependent Voigt model may improve the results, what is now difficult due to absence of speed-dependent Voigt spectroscopic data.

At this moment the precision of the method is not sufficient to obtain appropriate data for deuterium excess and further development of simultaneous remote atmospheric measurements of $\delta^{18}O$ and δD is particularly important for better understanding climate processes and atmospheric water cycle.

Acknowledgements. This research at Ural Federal University was supported by the grant of Russian government 11.G34.31.0064 (WSIBISO Project) and by the RFBR grant 12-01-00801-a. Financial support by the European Commission within the research project NORS is acknowledged.

References

- Anderson, G. P., Clough, S. A., Kneizys, F. X., Chetwynd, J. H., and Shettle, E. P.: AFGL atmospheric constituent profiles (0–120 km), AFGL-TR-0110, Environmental Research Paper 954, Air Force Geophysics Laboratory, 43 pp., 1986.
- Barber, R. J., Tennyson, J., Harris, G. J., and Tolchenov, R. N.: A high-accuracy computed water line list, *Mon. Not. R. Astron. Soc.*, 368, 1087–1094, 2006.
- Berrisford, P., Dee, D., Fielding, K., Fuentes, M., Källberg, P., Kobayashi, S., and Uppala, S.: ERA report series – the ERA-Interim archive Version 1.0, 2009.
- Boesch, H., Deutscher, N. M., Warneke, T., Byckling, K., Cogan, A. J., Griffith, D. W. T., Notholt, J., Parker, R. J., and Wang, Z.: HDO/H₂O ratio retrievals from GOSAT, *Atmos. Meas. Tech.*, 6, 599–612, doi:<http://dx.doi.org/10.5194/amt-6-599-2013>, 2013.
- Boone, C. D., Walker, K. A., and Bernath, P. F.: Speed-dependent Voigt profile for water vapor in infrared remote sensing applications, *J. Quant. Spectrosc. Ra.*, 105, 525–532, doi:<http://dx.doi.org/10.1016/j.jqsrt.2006.11.015>, 2007.
- Craig, H.: Standard for reporting concentrations of deuterium and oxygen-18 in natural waters, *Science*, 133, 1833–1834, 1961.
- Coffey, M. T., Hannigan, J. W., and Goldman, A.: Observations of upper tropospheric/lower stratospheric water vapour and its isotopologues, *J. Geophys. Res.*, 111, D14313, doi:<http://dx.doi.org/10.1029/2005JD006093>, 2006.
- Coudert, L. H., Wagner, G., Birk, M., Baranov, Yu. I., Lafferty, W. J., and Flaud, J.-M.: The H¹⁶O molecule: line position and line 2 intensity analyses up to the second triad, *J. Mol. Spectrosc.*, 251, 339–357, 2008.
- Dansgaard, W.: Stable isotopes in precipitation, *Tellus A*, 16, 4, doi:<http://dx.doi.org/10.3402/tellusa.v16i4.8993>, 1964.
- Dee, D. P., Uppala, S. M., Simmons, A. J., Berrisford, P., Poli, P., Kobayashi, S., Andrae, U., Balmaseda, M. A., Balsamo, G., Bauer, P., Bechtold, P., Beljaars, A. C. M., van de Berg, L., Bidlot, J., Bormann, N., Delsol, C., Dragani, R., Fuentes, M., Geer, A. J., Haimberger, L., Healy, S. B., Hersbach, H., Holm, E. V., Isaksen, L., Kallberg, P., Kohler, M., Matricardi, M., McNally, A. P., Monge-Sanz, B. M., Morcrette, J.-J., Park, B.-K., Peubey, C., de Rosnay, P., Tavolato, C., Thepaut, J.-N., and Vitart, F.: The ERA-Interim reanalysis: configuration and performance of the data assimilation system, *Q. J. Roy. Meteorol. Soc.*, 137, 553–597, 2011.
- ECMWF data server: available at: <http://data-portal.ecmwf.int/> (last access: 4 September 2013), 2013.
- Frankenberg, C., Yoshimura, K., Warneke, T., Aben, I., Butz, A., Deutscher, N., Griffith, D., Hase, F., Notholt, J., Schneider, M., Schrijver, H., and Röckmann, T.: Dynamic processes governing lower-

- tropospheric HDO/H₂O ratios as observed from space and ground, *Science*, 325, 1374–1377, doi:<http://dx.doi.org/10.1126/science.1173791>, 2009.
- 5 Frankenberg, C., Wunch, D., Toon, G., Risi, C., Scheepmaker, R., Lee, J.-E., Wennberg, P., and Worden, J.: Water vapor isotopologue retrievals from high-resolution GOSAT shortwave infrared spectra, *Atmos. Meas. Tech.*, 6, 263–274, doi:<http://dx.doi.org/10.5194/amt-6-263-2013>, 2013.
- Gribanov, K. G. and Zakharov, V. I.: Possibility to monitor the HDO/H₂O content ratio in the atmosphere from space observations of the outgoing thermal radiation, *Atmospheric and Ocean Optics*, 12, 825–826, 1999.
- 10 Gribanov, K. G., Zakharov, V. I., and Tashkun, S. A.: FIRE-ARMS software package and its application to passive IR sensing of the atmosphere, *Atmospheric and Ocean Optics*, 12, 358–361, 1999.
- Gribanov, K. G., Zakharov, V. I., Tashkun, S. A., and Tyuterev, V. G.: A new software tool for radiative transfer calculations and its application to IMG/ADEOS data, *J. Quant. Spectrosc. Ra.*, 68, 435–451, 2001.
- 15 Gribanov, K. G., Zakharov, V. I., Beresnev, S. A., Rokotyan, N. V., Poddubnyi, V. A., Imasu, R., Chistyakov, P. A., Skorik, G. G., and Vasin, V. V.: The sounding of HDO/H₂O in Ural’s atmosphere using ground-based measurements of IR-solar radiation with high spectral resolution, *Atmospheric and Ocean Optics*, 24, 124–127, 2011.
- Gribanov, K., Jouzel, J., Bastrikov, V., Bonne, J.-L., Breon, F.-M., Butzin, M., Cattani, O., Masson-Delmotte, V., Rokotyan, N., Werner, M., and Zakharov, V.: ECHAM5-wiso water vapour isotopologues simulation and its comparison with WS-CRDS measurements and retrievals from GOSAT and ground-based FTIR spectra in the atmosphere of Western Siberia, *Atmos. Chem. Phys. Discuss.*, 13, 2599–2640, doi:<http://dx.doi.org/10.5194/acpd-13-2599-2013>, 2013.
- 20 Gryazin, V., Risi, C., Jouzel, J., Kurita, N., Worden, J., Frankenberg, C., Bastrikov, V., Gribanov, K., and Stukova, O.: The added value of water isotopic measurements for understanding model biases in simulating the water cycle over Western Siberia, *Atmos. Chem. Phys. Discuss.*, submitted, 2013.
- Hagemann, S., Arpe, K., and Roeckner, E.: Evaluation of the hydrological cycle in the ECHAM5 model, *J. Climate*, 19, 3810–3827, 2006.
- Hannigan, J. W., Coffey, M. T., and Goldman, A.: Semi-autonomous FTS observation system for remote sensing of stratospheric and tropospheric gases, *J. Atmos. Ocean Tech.*, 26, 1814–1828, doi:<http://dx.doi.org/10.1175/2009JTECHA1230.1>, 2009.
- 30 Herbin, H., Hurtmans, D., Turquety, S., Wespes, C., Barret, B., Hadji-Lazaro, J., Clerbaux, C., and Coheur, P.-F.: Global distributions of water vapour isotopologues retrieved from IMG/ADEOS data,

Atmos. Chem. Phys., 7, 3957–3968, doi:<http://dx.doi.org/10.5194/acp-7-3957-2007>, 2007.

Herbin, H., Hurtmans, D., Clerbaux, C., Clarisse, L., and Coheur, P.-F.: H_2^{16}O and HDO measurements with IASI/MetOp, Atmos. Chem. Phys., 9, 9433–9447, doi:<http://dx.doi.org/10.5194/acp-9-9433-2009>, 2009.

Hoffmann, G., Werner, M., and Heimann, M.: Water isotope module of the ECHAM atmospheric general circulation model: a study on timescales from days to several years, J. Geophys. Res., 103, 16871–16896, doi:<http://dx.doi.org/10.1029/98JD004231>, 1998.

Jenouvrier, A., Daumont, L., Regalia-Jarlot, L., Tyuterev, V. G., Carleer, M., Vandaele, A. C., Mikhailenko, S., and Fally, S.: Fourier transform measurements of water vapor line parameters in the 4200–6600 cm^{-1} region, J. Quant. Spectrosc. Ra., 105, 326–355, 2007.

Jouzel, J., Russel, G., Suozzo, R., Kloster, R., White, J., and Broecker, W.: Simulations of the HDO and H_2^{18}O atmospheric cycles using the NASA GISS General Circulation Model: the seasonal cycle for present-day conditions, J. Geophys. Res., 92, 14739–14760, 1987.

Kalnay, E., Kanamitsu, M., Kistler, R., Collins, W., Deaven, D., Gandin, L., Iredell, M., Saha, S., White, G., Woollen, J., Zhu, Y., Leetmaa, A., Reynolds, R., Chelliah, M., Ebisuzaki, W., Higgins, W., Janowiak, J., Mo, K. C., Ropelewski, C., Wang, J., Jenne, R., and Joseph, D.: The NCEP/NCAR 40 yr reanalysis project, B. Am. Meteorol. Soc., 77, 437–471, 1996.

Keppel-Aleks, G., Toon, G. C., Wennberg, P. O., and Deutscher, N. M.: Reducing the impact of source brightness fluctuations on spectra obtained by Fourier-transform spectrometry, Appl. Optics, 46, 4774–4779, 2007.

Kerstel, E. R. T., van Trigt, R., Dam, N., Reuss, J., and Meijer, H. A. J.: Simultaneous determination of the $^2\text{H}/^1\text{H}$, $^{17}\text{O}/^{16}\text{O}$, and $^{18}\text{O}/^{16}\text{O}$, isotope abundance ratios in water by means of laser spectrometry, Anal. Chem., 71, 5297–5303, 1999.

Krishnamurti, T. N., Xue, J., Bedi, H. S., Ingles, K., and Oosterhof, D.: Physical initialization for numerical weather prediction over the tropics, Tellus A, 43, 53–81, doi:<http://dx.doi.org/10.1034/j.1600-0870.1991.t01-3-00007.x>, 1991.

Kuang, Z., Toon, G. C., Wennberg P. O., and Yung Y. L.: Measured HDO/H₂O ratios across the tropical tropopause, Geophys. Res. Lett., 30(7), 1–4, doi:10.1029/2003GL017023, 2003.

Langebroeck, P. M., Werner, M., and Lohmann, G.: Climate information imprinted in oxygen-isotopic composition of precipitation in Europe, Earth Planet. Sc. Lett., 311, 144–154, 2011.

Lee, X., Sargent, S., Smith, R., and Tanner, B.: In situ measurement of the water vapor o-18/o-16 isotope ratio for atmospheric and ecological applications, *J. Atmos. Ocean. Tech.*, 22, 1305–1305, doi:<http://dx.doi.org/10.1175/JTECH9001.1a10.1175/JTECH9001.1a>, 2005.

Merlivat, L. and Jouzel, J.: Global climatic interpretation of the deuterium-oxygen 18 relationship for precipitation, *J. Geophys. Res.*, 84, 5029, doi:<http://dx.doi.org/10.1029/JC084iC08p0502910.1029/JC084iC08p05029>, 1979.

Mikhailenko, S. N., Le, W., Kassi, S., and Campargue, A.: Weak water absorption lines around 1.455 and 1.66 μm by CW-CRDS, *J. Mol. Spectrosc.*, 244/2, 170–178, 2007.

Mikhailenko, S. N., Albert, K. A. K., Mellau, G., Klee, S., Winnewisser, B. P., Winnewisser, M., and Tyuterev, V. G.: Water vapor absorption line intensities in the 1900–6600 cm^{-1} region, *J. Quant. Spectrosc. Ra.*, 109, 2687–2696, 2008.

Moyer, E. J., Irion, F. W., Yung, Y. L., and Gunson, M. R.: ATMOS stratospheric deuterated water and implications for troposphere stratosphere transport, *Geophys. Res. Lett.*, 23, 2385–2388, 1996.

Nassar, R., Bernath, P. F., Boone, C. D., Gettelman, A., McLeod, S. D. and Rinsland, C. P.: Variability in HDO/H₂O abundance ratios in the tropical tropopause layer, *J. Geophys. Res.*, 112(D21), D21305, doi:10.1029/2007JD008417, 2007.

Noone, D. and Simmonds, I.: Associations between delta O-18 of water and climate parameters in a simulation of atmospheric circulation for 1979–95, *J. Climate*, 15, 3150–3169, 2002.

Pommier, M., Lacour, J.-L., Risi, C., Bréon, F.-M., Clerboux, C., Coheur, P.-F., Gribanov, K., Hurtmans, D., Jouzel, J., and Zakharov, V.: Observation of tropospheric δD by IASI over the Western Siberia: comparison with a GCM, *Atmos. Meas. Tech. Discuss.*, 6, 11055–11092, doi:<http://dx.doi.org/10.5194/amtd-6-11055-201310.5194/amtd-6-11055-2013>, 2013.

Payne, V. H., Noone, D., Dudhia, A., Piccolo, C., and Grainger, R. G.: Global satellite measurements of HDO and implications for understanding the transport of water vapour into the stratosphere, *Q. J. Roy. Meteor. Soc.*, 133, 1459–1471, doi:<http://dx.doi.org/10.1002/qj.12710.1002/qj.127>, 2007.

Rast, S.: Sea ice and nudging in ECHAM5, available at: <http://www.mpimet.mpg.de/en/staff/sebastian-rast/echam-special-documentation.html> (last access: 10 January 2014), 2008.

Rinsland, C. P., Gunson, M. R., Foster, J. C., Toth, R. A., Farmer, C. B., and Zander, R.: Stratospheric profiles of heavy water vapor isotopes and CH₃D from Analysis of the ATMOS Spacelab 3 infrared solar spectra, *J. Geophys. Res.*, 96, 1057–1068, 1991.

Risi, C., Bony, S., Vimeux, F., and Jouzel, J.: Water-stable isotopes in the LMDZ4 general circulation model: model evaluation for present-day and past climates and applica-

- tions to climatic interpretations of tropical isotopic records, *J. Geophys. Res.*, 115, 1–27, doi:<http://dx.doi.org/10.1029/2009JD013255>.1029/2009JD013255, 2010a.
- Risi, C., Bony, S., Vimeux, F., Frankenberg, C., Noone, D., and Worden, J.: Understanding the Sahelian water budget through the isotopic composition of water vapor and precipitation, *J. Geophys. Res.*, 115, D24110, doi:<http://dx.doi.org/10.1029/2010JD014690>.1029/2010JD014690, 2010b.
- 5 Risi, C., Noone, D., Worden, J., Frankenberg, C., Stiller, G., Kiefer, M., Funke, B., Walker, K., Bernath, P., Schneider, M., Wunch, D., Sherlock, V., Deutscher, N., Griffith, D., Wennberg, P. O., Strong, K., Smale, D., Mahieu, E., Barthlott, S., Hase, F., García, O., Notholt, J., Warneke, T., Toon, G., Sayres, D., Bony, S., Lee, J., Brown, D., Uemura, R., and Sturm, C.: Process-evaluation of tropospheric humidity simulated by general circulation models using water vapor isotopologues: 1. Comparison between models and observations, *J. Geophys. Res.*, 117, D05303, doi:<http://dx.doi.org/10.1029/2011JD016621>.1029/2011JD016621, 2012a.
- 10 Risi, C., Noone, D., Worden, J., Frankenberg, C., Stiller, G., Kiefer, M., Funke, B., Walker, K., Bernath, P., Schneider, M., Bony, S., Lee, J., Brown, D., and Sturm, C.: Process-evaluation of tropospheric humidity simulated by general circulation models using water vapor isotopic observations: 2. Using isotopic diagnostics to understand the mid and upper tropospheric moist bias in the tropics and subtropics, *J. Geophys. Res.*, 117, D05304, doi:<http://dx.doi.org/10.1029/2011JD016623>.1029/2011JD016623, 2012b.
- 15 Risi, C., Noone, D., Frankenberg, C., and Worden, J.: Role of continental recycling in intraseasonal variations of continental moisture as deduced from model simulations and water vapor isotopic measurements, *Water Resour. Res.*, 49, 1–21, doi:<http://dx.doi.org/10.1002/wrcr.20312>.1002/wrcr.20312, 2013.
- Rodgers, C. D.: *Inverse Methods for Atmospheric Sounding: Theory and Practice*, World Scientific, 2000.
- 20 Rothman, L. S., Gordon, I. E., Barbe, A., Benner, D. C., Bernath, P. F., Birk, M., Boudon, V., Brown, L. R., Campargue, A., and Champion, J. P.: The HITRAN 2008 molecular spectroscopic database, *J. Quant. Spectrosc. Ra.*, 110, 533–572, doi:<http://dx.doi.org/10.1016/j.jqsrt.2009.02.013>.1016/j.jqsrt.2009.02.013, 2009.
- 25 Rothman, L. S., Gordon, I. E., Babikov, Y., Barbe, A., Benner, D. C., Bernath, P. F., Birk, M., Biz-zocchi, L., Boudon, V., Brown, L. R., Campargue, A., Chance, K., Coudert, L. H., Devi, V. M., Drouin, B. J., Fayt, A., Flaud, J.-M., Gamache, R. R., Harrison, J., Hartmann, J.-M., Hill, C., Hodges, J. T., Jacquemart, D., Jolly, A., Lamouroux, J., LeRoy, R. J., Li, G., Long, D., Mackie, C. J., Massie, S. T., Mikhailenko, S., Müller, H. S. P., Naumenko, O. V., Nikitin, A. V., Orphal, J.,
- 30

- Perevalov, V. I., Perrin, A., Polovtseva, E. R., Richard, C., Smith, M. A. H., Starikova, E., Sung, K., Tashkun, S. A., Tennyson, J., Toon, G. C., Tyuterev, V. G., and Wagner, G.: The HITRAN 2012 Molecular Spectroscopic Database, *J. Quant. Spectrosc. Ra.*, Elsevier, ISSN 0022-4073, 2013.
- 5 Roeckner, E., Bäuml, G., Bonaventura, L., Brokopf, R., Esch, M., Giorgetta, M., Hagemann, S., Kirchner, I., Kornblüeh, L., Manzini, E., Rhodin, A., Schlese, U., Schulzweida, U., and Tompkins, A.: The atmospheric general circulation model ECHAM5, Part 1, Model description, Report No. 349, Max Planck Institute for Meteorology, Hamburg, Germany, 2003.
- Roeckner, E., Brokopf, R., Esch, M., Giorgetta, M., Hagemann, S., Manzini, E., Schlese, U., and Schulzweida, U.: Sensitivity of simulated climate to horizontal and vertical resolution in the ECHAM5 atmosphere model, *J. Climate*, 19, 3771–3791, 2006.
- 10 Rozanski, K., Araguás-Araguás, L., and Gonfiantini, R.: Relation between long-term trends of oxygen-18 isotope composition of precipitation and climate, *Science*, 258, 981–985, 1992.
- Shillings, A. J. L., Ball, S. M., Barber, M. J., Tennyson, J., and Jones, R. L.: An upper limit for water dimer absorption in the 750 nm spectral region and a revised water line list, *Atmos. Chem. Phys.*, 11, 4273–4287, doi:<http://dx.doi.org/10.5194/acp-11-4273-2011>, 2011.
- 15 Schneider, M. and Hase, F.: Optimal estimation of tropospheric H₂O and δ D with IASI/METOP, *Atmos. Chem. Phys.*, 11, 11207–11220, doi:<http://dx.doi.org/10.5194/acp-11-11207-2011>, 2011.
- Schneider, M., Hase, F., and Blumenstock, T.: Ground-based remote sensing of HDO/H₂O ratio profiles: introduction and validation of an innovative retrieval approach, *Atmos. Chem. Phys.*, 6, 4705–4722, doi:<http://dx.doi.org/10.5194/acp-6-4705-2006>, 2006.
- 20 Schneider, M., Toon, G. C., Blavier, J.-F., Hase, F., and Leblanc, T.: H₂O and δ D profiles remotely sensed from ground in different spectral infrared regions, *Atmos. Meas. Tech.*, 3, 1599–1613, doi:<http://dx.doi.org/10.5194/amt-3-1599-2010>, 2010.
- 25 Schneider, M., Hase, F., Blavier, J. F., Toon, G. C., and Leblanc, T.: An empirical study on the importance of a speed-dependent Voigt line shape model for tropospheric water vapor profile remote sensing, *J. Quant. Spectrosc. Ra.*, 112, 465–474, doi:<http://dx.doi.org/10.1016/j.jqsrt.2010.09.008>, 2011.
- Schneider, M., Barthlott, S., Hase, F., González, Y., Yoshimura, K., García, O. E., Sepúlveda, E., Gomez-Pelaez, A., Gisi, M., Kohlhepp, R., Dohe, S., Blumenstock, T., Wiegeler, A., Christner, E., Strong, K., Weaver, D., Palm, M., Deutscher, N. M., Warneke, T., Notholt, J., Lejeune, B., Demoulin, P., Jones, N., Griffith, D. W. T., Smale, D., and Robinson, J.: Ground-based remote sens-
- 30

- ing of tropospheric water vapour isotopologues within the project MUSICA, *Atmos. Meas. Tech.*, 5, 3007–3027, doi:<http://dx.doi.org/10.5194/amt-5-3007-2012>, 2012.
- Skorik, G. G., Vasin, V. V., Griбанov, K. G., Jouze, L. J., Zakharov, V. I., and Rokotyan, N. V.: Retrieval of vertical profiles of water vapour isotopologues in the atmosphere using infrared transmission spectra of solar radiation, *Academy of Science Reports*, in press, 2014.
- Steen-Larsen, H. C., Johnsen, S. J., Masson-Delmotte, V., Stenni, B., Risi, C., Sodemann, H., Balslev-Clausen, D., Blunier, T., Dahl-Jensen, D., Ellehøj, M. D., Falourd, S., Grindsted, A., Gkinis, V., Jouzel, J., Popp, T., Sheldon, S., Simonsen, S. B., Sjolte, J., Steffensen, J. P., Sperlich, P., Sveinbjörnsdóttir, A. E., Vinther, B. M., and White, J. W. C.: Continuous monitoring of summer surface water vapor isotopic composition above the Greenland Ice Sheet, *Atmos. Chem. Phys.*, 13, 4815–4828, doi:<http://dx.doi.org/10.5194/acp-13-4815-2013>, 2013.
- Tolchenov, R. and Tennyson, J.: Water line parameters from refitted spectra constrained by empirical upper state levels: study of the 9500–14500 cm^{-1} region, *J. Quant. Spectrosc. Ra.*, 109, 559–568, doi:<http://dx.doi.org/10.1016/j.jqsrt.2007.08.001>, 2008.
- Uppala, S. M., Kållberg, P. W., Simmons, A. J., Andrae, U., da Costa Bechtold, V., Fiorino, M., Gibson, J. K., Haseler, J., Hernandez, A., Kelly, G. A., Li, X., Onogi, K., Saarinen, S., Sokka, N., Allan, R. P., Andersson, E., Arpe, K., Balmaseda, M. A., Beljaars, A. C. M., van de Berg, L., Bidlot, J., Bormann, N., Caires, S., Chevallier, F., Dethof, A., Dragosavac, M., Fisher, M., Fuentes, M., Hagemann, S., Hólm, E., Hoskins, B. J., Isaksen, I., Janssen, P. A. E. M., Jenne, R., McNally, A. P., Mahfouf, J.-F., Morcrette, J.-J., Rayner, N. A., Saunders, R. W., Simon, P., Sterl, A., Trenberth, K. E., Untch, A., Vasiljevic, D., Viterbo, P., and Woollen, J. 2005: The ERA-40 re-analysis, *Q. J. Roy. Meteorol. Soc.*, 131, 2961–3012, 2005.
- Werner, M., Heimann, M., and Hoffmann, G.: Isotopic composition and origin of polar precipitation in present and glacial climate simulations, *Tellus B*, 53, 53–71, 2001.
- Werner, M., Langebroek, P. M., Carlsen, T., Herold, M., and Lohmann, G.: Stable water isotopes in the ECHAM5 general circulation model: toward highresolution isotope modeling on a global scale, *J. Geophys. Res.*, 16, D15109, doi:<http://dx.doi.org/10.1029/2011JD015681>, 2011.
- Worden, J., Bowman, K., Noone, D., Beer, R., Clough, S., Eldering, A., Fisher, B., Goldman, A., Gunson, M., Herman, R., Kulawik, S. S., Lampel, M., Luo, M., Osterman, G., Rinsland, C., Rodgers, C., Sander, S., Shephard, M., and Worden, H.: Tropospheric emission spectrometer observations of the tropospheric HDO/H₂O ratio: estimation approach and characterization, *J. Geophys. Res.*, 111, D16309, doi:<http://dx.doi.org/10.1029/2005JD006606>, 2006.

- Worden, J., Noone, D., Bowman, K., Beer, R., Eldering, A., Fisher, B., Gunson, M., Goldman, A., Herman, R., Kulawik, S. S., Lampel, M., Osterman, G., Rinsland, C., Rodgers, C., Sander, C., Shephard, M., Webster, C. R., and Worden, H.: Importance of rain evaporation and continental convection in the tropical water cycle, *Nature*, 445, 528–532, doi:<http://dx.doi.org/10.1038/nature05508>, 2007.
- 5 Wunch, D., Toon, G. C., Wennberg, P. O., Wofsy, S. C., Stephens, B. B., Fischer, M. L., Uchino, O., Abshire, J. B., Bernath, P., Biraud, S. C., Blavier, J.-F. L., Boone, C., Bowman, K. P., Browell, E. V., Campos, T., Connor, B. J., Daube, B. C., Deutscher, N. M., Diao, M., Elkins, J. W., Gerbig, C., Gottlieb, E., Griffith, D. W. T., Hurst, D. F., Jiménez, R., Keppel-Aleks, G., Kort, E. A., Macatangay, R., Machida, T., Matsueda, H., Moore, F., Morino, I., Park, S., Robinson, J., Roehl, C. M., Sawa, Y., Sherlock, V., Sweeney, C., Tanaka, T., and Zondlo, M. A.: Calibration of the Total Carbon Column Observing Network using aircraft profile data, *Atmos. Meas. Tech.*, 3, 1351–1362, doi:<http://dx.doi.org/10.5194/amt-3-1351-2010>, 2010.
- 10 Wunch, D., Toon, G. C., Blavier, J.-F. L., Washenfelder, R. A., Notholt, J., Connor, B. J., Griffith, D. W. T., Sherlock, V., and Wennberg, P. O.: The total carbon column observing network, *Philos. T. R. Soc. A*, 369, 2087–2112, 2011.
- Yoshimura, K., Kanamitsu, M., Noone, D., and Oki, T.: Historical isotope simulation using reanalysis atmospheric data, *J. Geophys. Res.*, 113, 1–15, doi:<http://dx.doi.org/10.1029/2008JD010074>, 2008.
- 20 Zakharov, V. I., Imasu, R., Gribanov, K. G., Hoffmann, G., and Jouzel, J.: Latitudinal distribution of the deuterium to hydrogen ratio in the atmospheric water vapor retrieved from IMG/ADEOS data, *Geophys. Res. Lett.*, 31, L12104, doi:<http://dx.doi.org/10.1029/2004GL019433>, 2004.

Table 1. Summarized information about spectral windows used for the retrieval of $\delta^{18}\text{O}$ and δD . Windows marked by “*” are used in the TCCON community table

Molecule	Center, cm^{-1}	Width, cm^{-1}	Interfering Species
H_2^{18}O	4056.50	1.0	H_2^{16}O CO_2 CH_4
H_2^{18}O	4062.75	1.0	H_2^{16}O CO_2 CH_4
H_2^{18}O	4067.50	2.0	H_2^{16}O CO_2 CH_4
H_2^{18}O	4090.50	1.0	H_2^{16}O CO_2 CH_4
H_2^{18}O	4115.25	1.5	H_2^{16}O CO_2 CH_4
H_2^{18}O	5012.25	1.5	H_2^{16}O CO_2 CH_4
H_2^{18}O	5076.90	0.6	H_2^{16}O CO_2 CH_4
H_2^{18}O	6656.25	1.0	H_2^{16}O CO_2 CH_4
H_2^{18}O	6739.30	2.5	H_2^{16}O H_2^{17}O
H_2^{18}O	6740.20	1.0	H_2^{16}O H_2^{17}O
H_2^{18}O	6772.40	0.7	H_2^{16}O HDO
H_2^{18}O	6845.00	2.5	H_2^{16}O CO_2 CH_4
H_2^{18}O	6858.00	2.0	H_2^{16}O CO_2 CH_4
H_2^{18}O	6889.50	1.5	H_2^{16}O CO_2 CH_4
H_2^{18}O	6927.50	1.5	H_2^{16}O CO_2 CH_4
H_2^{18}O	7030.00	2.0	H_2^{16}O CO_2 CH_4
HDO	4038.00	2.0	H_2^{16}O HF OCS O_3
HDO	4054.60	3.3	H_2^{16}O CH_4 *
HDO	4100.36	0.9	H_2^{16}O CH_4 OCS
HDO	4116.10	8.0	H_2^{16}O OCS *
HDO	4144.50	0.8	H_2^{16}O CH_4
HDO	4157.70	1.2	H_2^{16}O CH_4
HDO	4212.45	1.9	H_2^{16}O CH_4 *
HDO	4232.50	11.0	H_2^{16}O CH_4 *
HDO	5058.95	0.6	H_2^{16}O CO_2
HDO	6330.05	45.5	H_2^{16}O CO_2 *
HDO	6377.40	50.2	H_2^{16}O CO_2 *
H_2^{16}O	4259.57	1.0	HDO CH_4
H_2^{16}O	4504.98	1.0	CH_4
H_2^{16}O	4514.00	6.0	CH_4
H_2^{16}O	4523.50	2.0	CH_4
H_2^{16}O	4546.87	1.0	CH_4

Table 1. Continued.
table

Molecule	Center, cm^{-1}	Width, cm^{-1}	Interfering Species	
H_2^{16}O	4552.00	2.5	CH_4	
H_2^{16}O	4556.20	2.0	CH_4	
H_2^{16}O	4565.20	2.5	CO_2 CH_4	*
H_2^{16}O	4571.75	2.5	CO_2 CH_4	*
H_2^{16}O	4576.85	1.9	CH_4	*
H_2^{16}O	4601.77	1.0	CO_2 CH_4	
H_2^{16}O	4609.45	1.0	CO_2 CH_4	
H_2^{16}O	4611.05	2.2	CH_4	*
H_2^{16}O	4622.00	2.3	CO_2	*
H_2^{16}O	4645.00	30.0	CO_2 CH_4	
H_2^{16}O	4681.93	1.0		
H_2^{16}O	4699.55	4.0	N_2O	*
H_2^{16}O	4706.43	1.0		
H_2^{16}O	4811.56	1.0	CO_2	
H_2^{16}O	4848.03	1.0	CO_2	
H_2^{16}O	4893.14	1.0	CO_2	
H_2^{16}O	5056.98	1.0	CO_2 HDO	
H_2^{16}O	5084.27	1.0	H_2^{18}O CO_2	
H_2^{16}O	5619.16	1.0		
H_2^{16}O	5696.16	1.0	CH_4	
H_2^{16}O	5741.13	1.0	CH_4	
H_2^{16}O	6034.2	1.7	CO_2 CH_4	
H_2^{16}O	6047.79	1.0	CO_2	
H_2^{16}O	6076.90	3.85	HDO CO_2 CH_4	*
H_2^{16}O	6099.35	1.0	CO_2	*
H_2^{16}O	6125.85	1.5	CO_2 CH_4	*
H_2^{16}O	6177.30	0.8	CO_2 CH_4	*
H_2^{16}O	6185.68	1.0	HDO CO_2 CH_4	
H_2^{16}O	6255.95	3.6	HDO CO_2	*
H_2^{16}O	6301.35	7.9	HDO CO_2	*
H_2^{16}O	6392.45	3.1	HDO	*
H_2^{16}O	6401.15	1.2	HDO	*
H_2^{16}O	6469.60	3.5	HDO CO_2	*
H_2^{16}O	6486.52	1.0	HDO CO_2	
H_2^{16}O	6604.51	1.0		

Table 2. Summarized information from the different uncertainty sources

	Measurement noise	1 % uncertainty in the temperature profile	15 % uncertainty in a priori H ₂ ¹⁶ O profile	5 % uncertainty in line intensities	2 % uncertainty in air broadened half width	15 % uncertainty in the coefficient of temperature dependence	SUM
δD	1‰	3‰	8‰	up to 12‰	up to 1.5‰	up to 4‰	29.5‰
$\delta^{18}\text{O}$	2‰	10‰	6‰	up to 2‰	up to 1‰	up to 5‰	26‰

2a

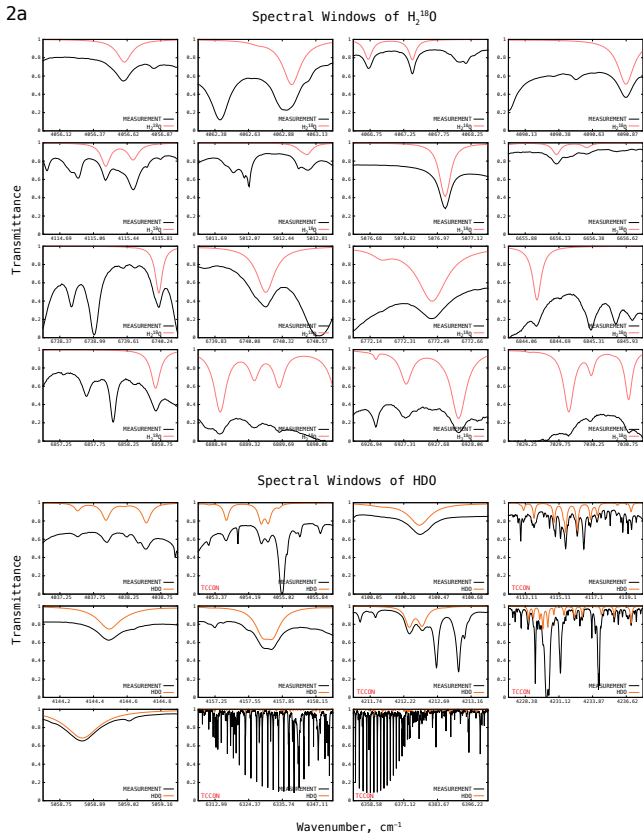


Fig. 1a. Refined set of spectral windows for H_2^{18}O and HDO retrieval. Black line: measurement; red and orange lines: signals of H_2^{18}O and HDO respectively. “TCCON” inscription indicates spectral windows used by the TCCON community.

2b

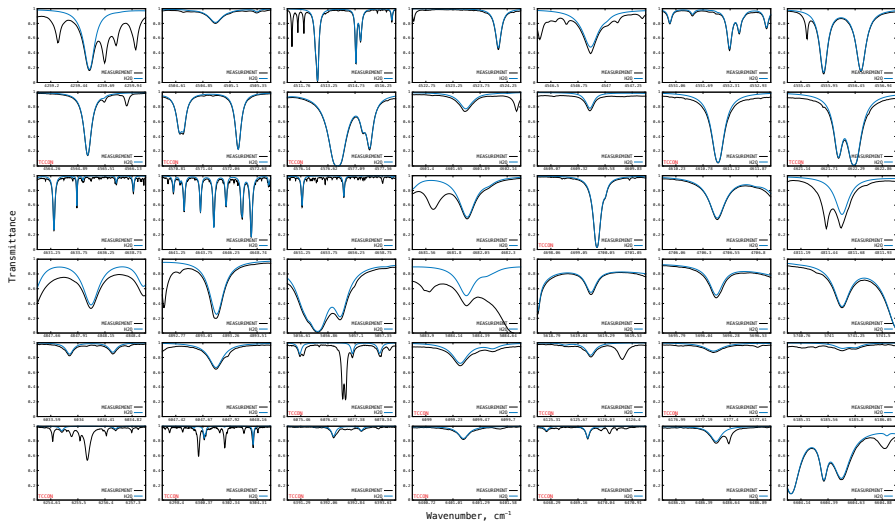
Spectral windows of H₂¹⁶O

Fig. 1b. The same as Fig. 2a, but for H₂¹⁶O.

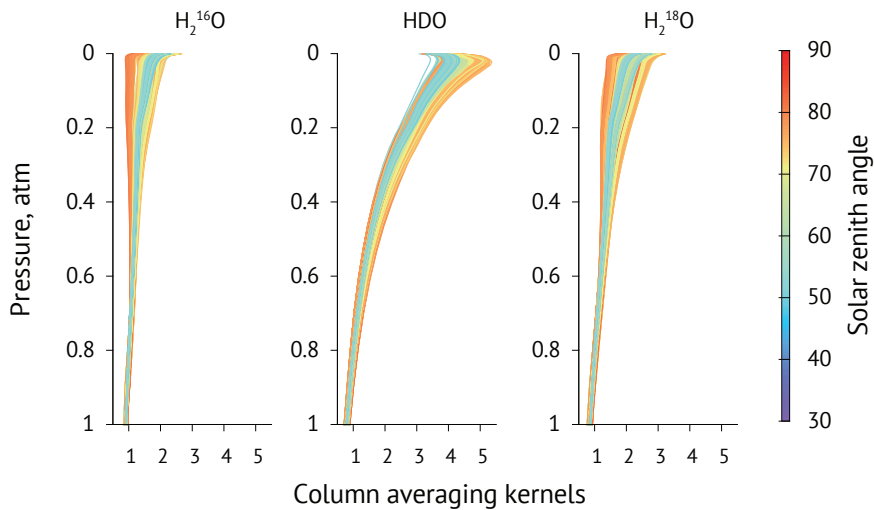


Fig. 2. Column averaging kernels of H_2^{16}O , HDO and H_2^{18}O .

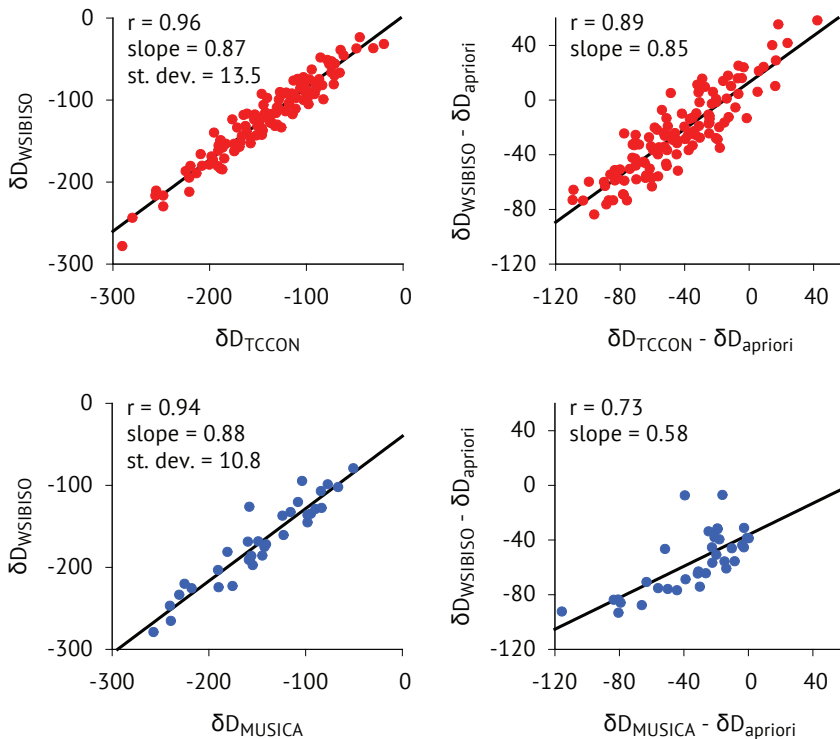


Fig. 3. Daily-averaged δD obtained from publicly available TCCON (a posteriori calculated, varying a priori) and MUSICA/NDACC (optimally estimated, single a priori) retrievals vs. δD obtained by using the refined set of spectral windows ($\delta D_{\text{WSIBISO}}$)

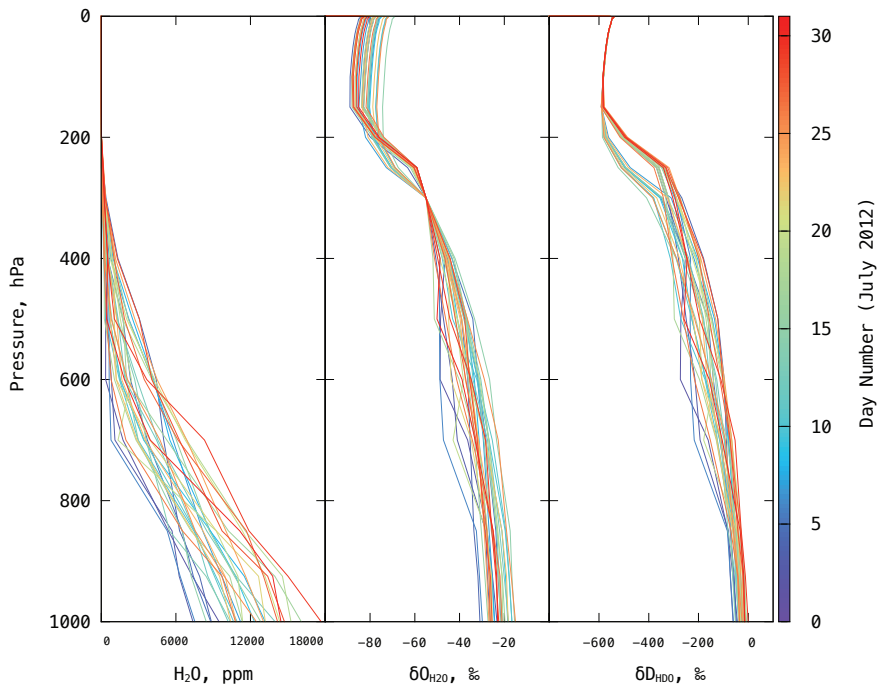


Fig. 4. Example of H₂O, δO_{H_2O} and δD_{HDO} initial guess profiles derived from NCEP/NCAR reanalysis data.

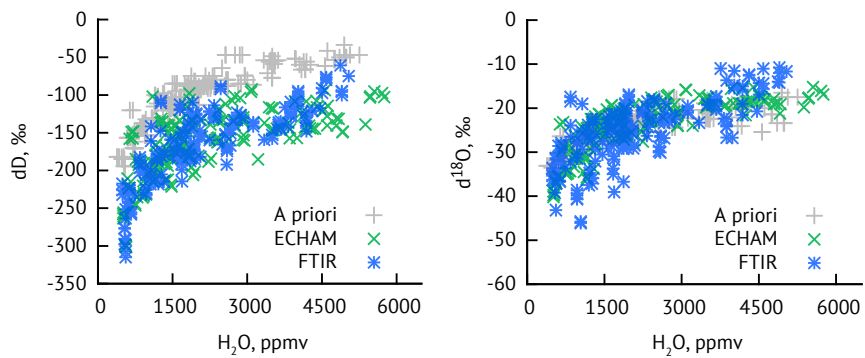


Fig. 5. Variations in columnar δD and $\delta^{18}O$.

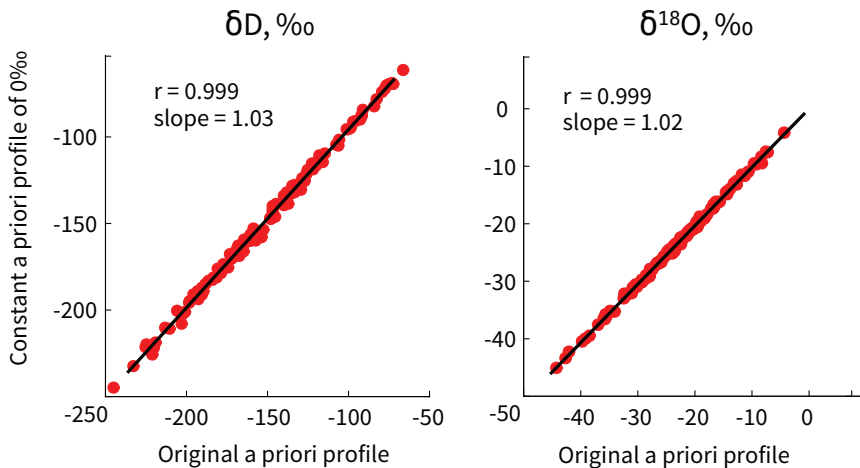


Fig. 6. Sensitivity of the retrieval to the shape of a priori profiles. Results obtained using constant $\delta^{18}O$ and δD profiles of 0‰ vs. results obtained with $H_2^{18}O$ and HDO a priori profiles calculated by Eqs. (2) and (3).

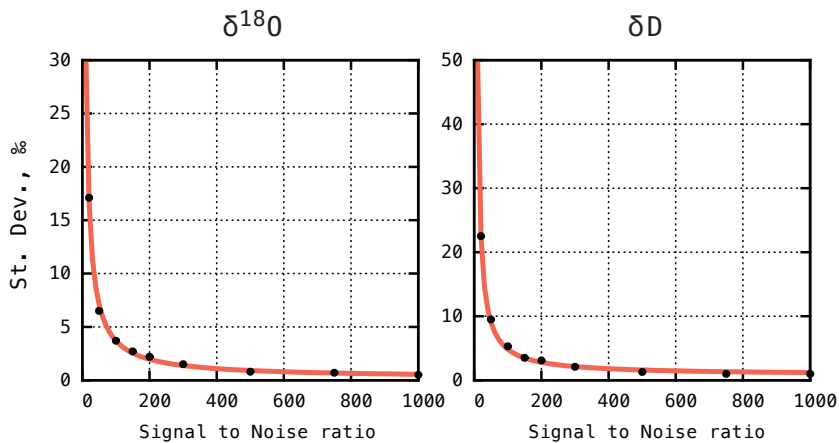


Fig. 7. Precision of the retrieval as a function of the signal to noise ratio of the measurement.

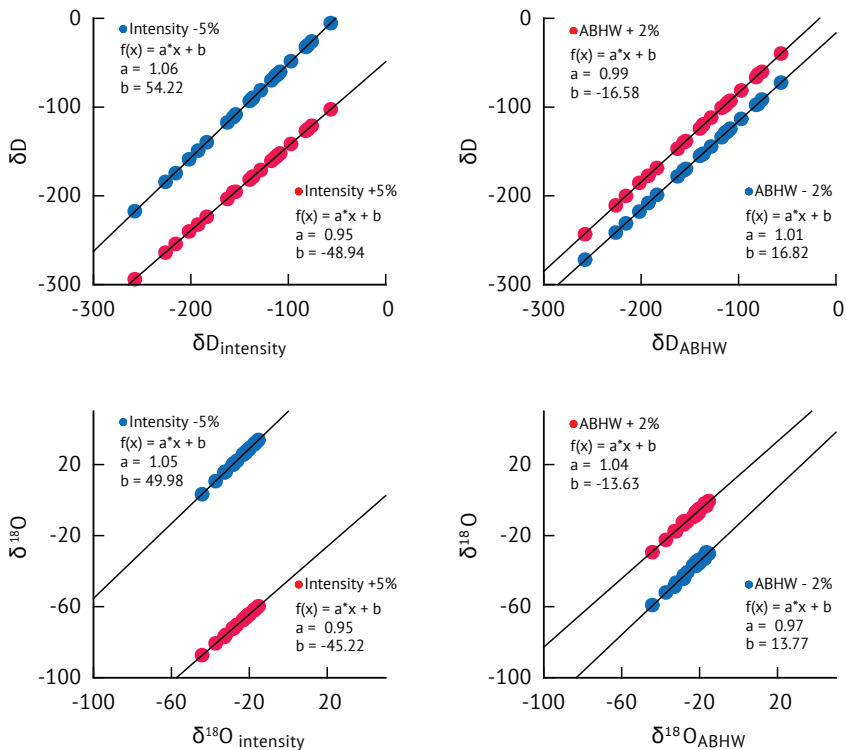


Fig. 8. Change in δD and $\delta^{18}O$ due to a change of spectroscopic line intensities by $\pm 5\%$ (left panels), due to a change of air broadened half width (ABHW) by $\pm 2\%$ (right panels).

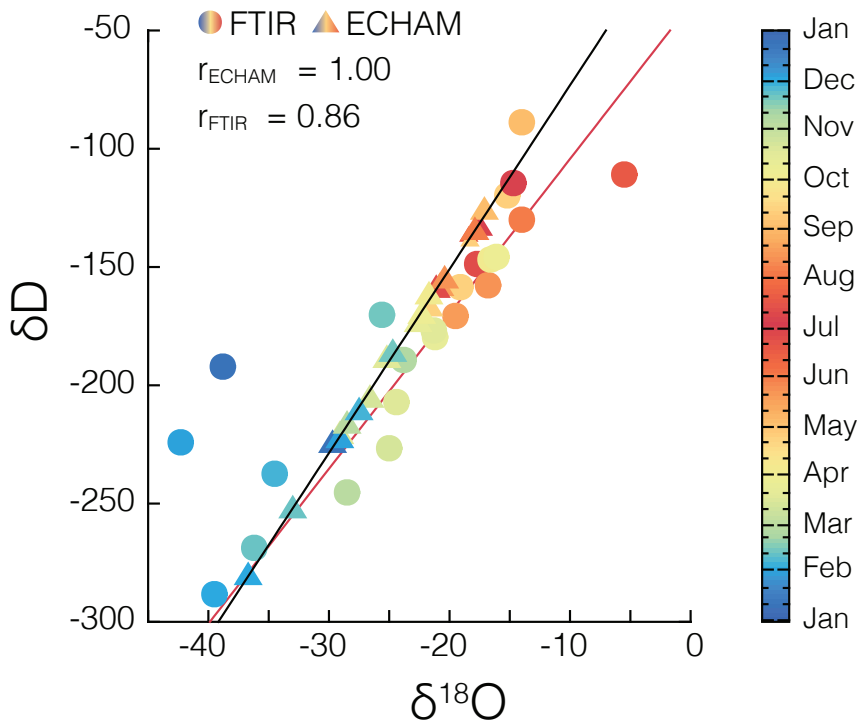


Fig. 9. Scatter plot of the retrieved (color dots) and simulated (color triangles) columnar values of $\delta^{18}\text{O}$ and δD .

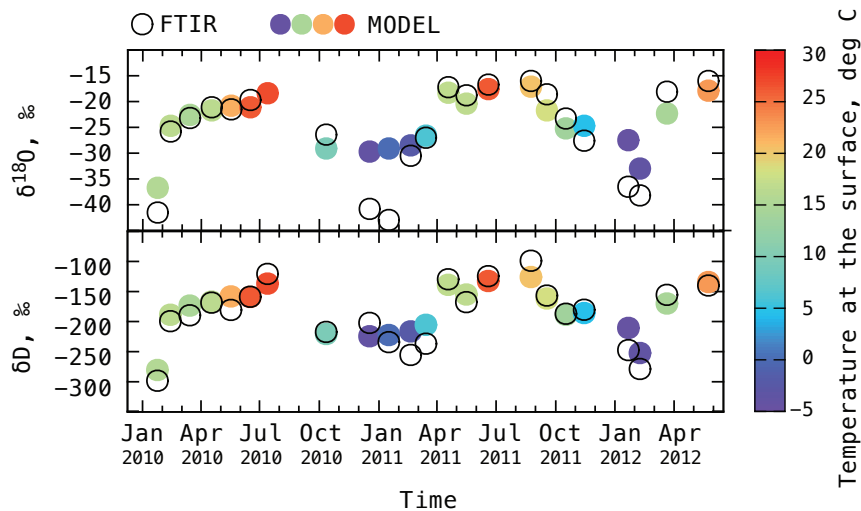


Fig. 10. Retrieved values of $\delta^{18}\text{O}$ and δD averaged during each month of measurements and corresponding ECHAM5-wiso model values.

Monthly averaged

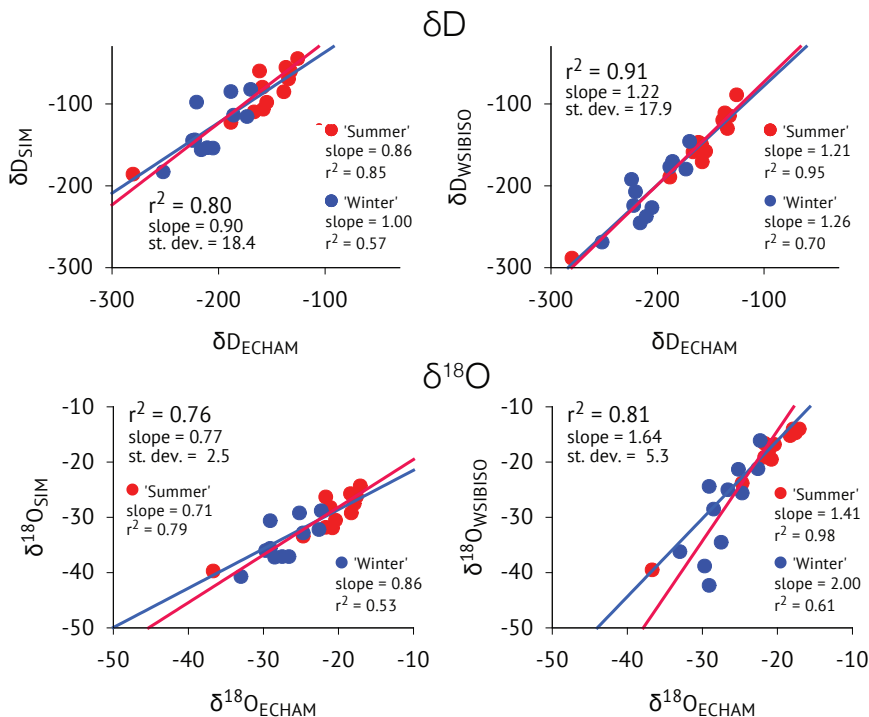


Fig. 11. Left panels: correlation between ECHAM5-*visu* model values and δD and $\delta^{18}O$ values calculated from the retrieved $H_2^{16}O$ using known relationships. Right panels: correlation between ECHAM5-*visu* model values and a posteriori calculated $\delta^{18}O$ ($\delta^{18}O_{WSIBISO}$) and δD ($\delta D_{WSIBISO}$). “Summer” red points correspond to surface air temperatures above 15 °C, “winter” blue points correspond to temperatures below 15 °C.